Measurement of the degree of spatial coherence of high-order harmonics using a Fresnel-mirror interferometer

L. Le Déroff,[1] P. Salières,[1] B. Carré,[1] D. Joyeux,[2] and D. Phalippou[2]
[1]*CEA, DSM/DRECAM/SPAM, Centre d'Etudes de Saclay, 91191 Gif-sur-Yvette, France*
[2]*Institut d'Optique Théorique et Appliquée, 91403 Orsay, France*
(Received 16 July 1999; published 3 March 2000)

We have studied in detail the spatial coherence of the far field of the 13th harmonic from a Ti:sapphire laser generated in xenon, as a function of the generation parameters. Experimentally, we use Fresnel mirrors to produce two-dimensional interferograms. This technique allows us to probe the coherence at different scales $d=1-3$ mm between the interfering rays, i.e., throughout the full section of the incident beam. A high uniform degree of mutual coherence γ_d, larger than 0.5 in most cases, is measured as a function of the position of the jet relative to the focus, and pressure in the jet. It confirms the high intrinsic spatial coherence already reported for the extreme-ultraviolet harmonics, which is much larger than the one produced from x-ray lasers. Spatial coherence decreases when the laser focus is moved toward the jet, and when the pressure is increased: the onset of ionization, as well as the intensity-dependent phase of the nonlinear polarization, are rapidly varying factors in time and space which degrade the correlation between the fields at two different points. Simulation of the coherence degree emphasizes the role of the intensity-dependent phase in the evolution of the coherence degree.

PACS number(s): 42.65.Ky, 42.25.Kb, 42.25.Hz

I. INTRODUCTION

High-order harmonic generation provides an efficient source of radiation in the extreme-ultraviolet (XUV) region, with rather unique characteristics. The most remarkable of these are the very short pulse duration and the spatial and temporal coherence. The detailed characterization of the harmonic light serves a double purpose. First, it reveals the complex underlying physics of the harmonic generation. Then it qualifies harmonic light in terms of a usable source for the applications. The two purposes are bound, since a good knowledge of the process now permits one to control and shape harmonic beam parameters such as the duration and the spectral and spatial distributions. The temporal and spatial coherence of the light is actually of great importance for the applications. On the one hand, the temporal coherence would allow, in principle, interferometry experiments using amplitude division. On the other hand, the spatial coherence grounds the possibility of interferometry using a wave-front division [1]. The high instantaneous brightness and the short pulse duration of the harmonic radiation should allow one to perform time-resolved, single-shot interferometry measurements in, for instance, high-density ionized media or thin solid films.

The study of the spatial properties of harmonic radiation first concentrated on a characterization of the far-field emission profiles. Peatross and Meyerhofer [2] and Tisch *et al.* [3] observed distorted profiles attributed to the effects of the intrinsic dipole phase and the ionization of the generating medium, respectively Salières *et al.* [4] showed that under some focusing conditions, very regular near-Gaussian angular distributions could be obtained. In particular, a transition from a centered profile to an annular profile could be observed by moving the laser focus position from before the gas jet to inside [5]. This evolution was interpreted by the change of phase matching in the medium, due to the interplay between the intrinsic dipole phase and the geometrical phase shift at the focus. The study of the far-field profiles is not sufficient to characterize the beam quality fully. Recently we measured the spot size of a harmonic beam in the focal region of a multilayer spherical mirror together with its far-field profile [6]. Good quality beams, diffraction limited nearly two times, are obtained at low pressure and small medium length, but degradation is observed when the pressure or the medium length is increased.

Spatial coherence is related to the correlation of the temporal fluctuations of the electromagnetic fields inside the beam; in other words, it is related to their ability to interfere. This is thus a field property distinct from the close-to-Gaussian character, which results in the possible focusing of the beam down to the diffraction limit. Actually, a close-to-Gaussian field should present a good spatial coherence, but the reciprocal is not true in general.

The spatial coherence of the harmonics is expected to be high, since they build up coherently in the generating medium from the highly coherent driving field. However, several factors involved are strongly time and space dependent. The intrinsic dipole phase which enters the nonlinear polarization depends directly on the laser intensity [7]. Moreover, at an intensity close to the saturation intensity, ionization takes place, i.e., a time- and space-dependent electron density develops in the medium. As a result, the ''building history'' of the harmonic field varies across the transverse section of the beam at the medium exit, and the spatial coherence should subsequently be reduced.

So far, the only measurements of the spatial coherence were reported by Ditmire *et al.* [8,9]. With a Young two-slit experiment they investigated the coherence of harmonics 11 to 19 of a frequency-doubled Nd: glass laser focused in helium. The coherence was measured quite close to the focus, since the slit pair was placed 40 mm away from the

gas jet. A slit spacing between 25 and 100 μm was used to probe the coherence inside the 200-μm full width at half maximum harmonic profiles. The observed good fringe visibility indicates a high spatial coherence that is strongly degraded at high intensity. The authors attributed this degradation to the free-electron dispersion introduced by the ionization of the medium. However, they did not find any significant change of the fringe visibility when changing the backing pressure, which is quite surprising since the free-electron dispersion should be all the more important as the pressure is high. The authors invoked the fact that harmonics may be efficiently generated *before* the maximum electron density is reached, so that the effective free-electron density ''seen'' by the harmonics may not change when changing the backing pressure. Another puzzling trend is the change of the fringe visibility when moving the center of the slit pair across the harmonic beam. The visibility increases from 0.4 for the slits centered to 0.7 near the edge of the beam. The coherence would thus change significantly inside the beam.

In this paper, we report systematic studies of the spatial coherence of the 13th and, to a lesser extent, the 15th harmonics produced in xenon from a Ti:sapphire laser at 800 nm. We have measured the degree of spatial coherence 1.3 m away from the generating medium, i.e., in a region where this coherence could be used in applications. We use a Fresnel-mirrors interferometer [10] (described in Sec. II), a system that allows us to probe simultaneously the spatial coherence in the beam between all the pairs of rays distant of a given distance d in the transverse section of the incident beam. The interference pattern can be read as a full-size, single-shot mapping of the spatial coherence throughout the beam, for a fixed distance d between the interfering rays. In contrast, with the Young slit system, only two rays separated by d interfere. A complete mapping of the coherence thus requires that the slits are moved throughout the beam section and, therefore, a single-shot picture is no longer measurable. Another advantage of the Fresnel-mirror setup is that the distance d is easily changed by simply changing the distance between the interferometer and the detector. By moving the detector away from the interferometer from 1 to 3 m, we have probed the coherence inside the beam at distances d between 1 and 3 mm. As a drawback, this technique introduces diffraction by the mirror central edge. In order to resolve the diffraction from the interference effects, we have developed an analysis, described in Sec. III, that extracts the degree of coherence γ_d from the interferograms. The results are presented in Sec. IV. The two-dimensional mapping shows a rather uniform degree of coherence γ_d. A relatively high average value, $\gamma_d \geqslant 0.5$, is measured for distance d as large as 2 mm, of the order of the beam section diameter. This is larger by at least one order of magnitude than the coherence of the field emitted by an incoherent source of the same diameter at focus. The γ_d degree is found to decrease significantly when the backing pressure is increased and when the gas jet is placed close to the laser focus. Finally, the variations of γ_d with the focusing conditions and the gas jet pressure are compared with simulations of the harmonic spatial coherence. This shows that ionization, that is space- and time-dependent conditions for the generation and the propagation of the harmonic field, degrades the spatial coherence, as reported in Ref. [9]. Moreover, the intensity-dependent, atomic dipole phase may equally play a role in the observed behavior.

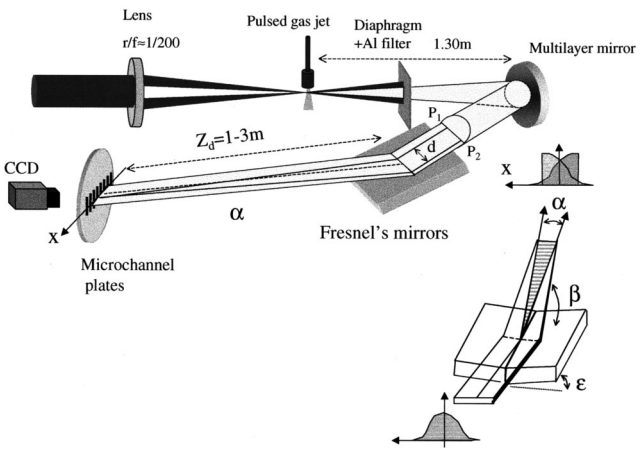

FIG. 1. Experimental setup. An annular shaped IR beam is used to generate harmonics on the axis; it is cut on a diaphragm of diameter 3.5 mm and a 100-nm aluminum filter. The 13th and 15th harmonics are reflected and collimated to a parallel beam of diameter 3–4 mm by a highly polished spherical multilayer mirror. The geometry of the Fresnel mirrors is detailed in the inset—see the angle values in the text. From the beam cross section before the interferometer, only a strip of the harmonic beam is sketched with a pair of parallel rays (defined by P_1 and P_2). All the rays separated by d in the incident beam interfere at a distance $Z_d = \alpha d$ from the interferometer. The detector is tilted to obtain sufficient resolution.

II. EXPERIMENTAL SETUP: FRESNEL's MIRROR INTERFEROMETER

The experimental setup is schematized in Fig. 1. The laser is an amplified Ti:sapphire system that delivers 60-fs pulses at 800 nm, of as much as 100 mJ of energy, with a 20-Hz repetition rate (IR beam); it is installed at the Laser Ultra-Court Accordable laser facility of the CEA/DRECAM in Saclay. A ring-shaped IR beam ($<$10 mJ; numerical aperture $r/f = 1/200$) is focused in a xenon gas jet at an intensity of 10^{13}–10^{14} W/cm^2 and then cut when it diverges at 1 m from the focus on a circular diaphragm of diameter 3.5 mm. This allows one to get rid of most of the intense laser beam, whereas the harmonics, that are mainly emitted on the axis, pass the diaphragm. To select one harmonic or a few harmonics, we use a Mo/Si multilayer mirror and a self-supported 100-nm aluminum foil. Harmonics 13 and 15 are the main components of the transmitted light through the system (referred to as $H13$ and $H15$, respectively). The harmonic source is placed at the focus of the multilayer mirror ($f = 1300$ mm), so that the collimated XUV beam is reflected parallel, under a full deviation of 14°, toward the interferometer located 2.6 m away. The harmonic profile is very regular, close to Gaussian, with a full width at $1/e^2$ around 3 mm, depending on the generating conditions. The Fresnel mirrors consist of two plane, highly polished, silica half-mirrors, which are tilted at $\varepsilon = 5.44$ mrad around their common straight edges. The harmonic beam, incoming

parallel to and centered on the mirror edge, is reflected at a grazing incidence $\beta = 94$ mrad on the two half-mirrors. Two reflected half-beams therefore cross under angle $\alpha = 2\beta\varepsilon \approx 1$ mrad and overlap, generating interference patterns. Thus rays that interfere at a given distance Z_d after the interferometer are *all the pairs of rays*, respectively, at P_1 and P_2 in the transverse section of the incident beam, where P_1 and P_2 vary in the transverse section but satisfy the following conditions: (i) The P_1P_2 segment is perpendicular to the vertical plane of incidence, i.e., P_1P_2 horizontal. (ii) The distance $d = P_1P_2$ is equal to αZ_d, an upper bound being the beam diameter of 3 mm. If we place a two-dimensional (2D) detector at a distance Z_d, we measure a 2D interferogram in which each point corresponds to a pair of interfering rays in the incident beam. Therefore, the 2D interferogram can be read as a map of the spatial coherence throughout the beam. This shows an obvious advantage of this technique over the Young two-slit technique, as we recalled in Sec. I. By changing the distance Z_d between 1 and 3 m, we can probe the transverse coherence of the beam at different distances $d = 1-3$ mm. The fringe spacing $i = \lambda/\alpha \approx \lambda Z_d/d$ depends only on the wavelength, so that the interferograms can be measured with the same resolution for different Z_d's. The fringe spacing is 60 μm for $H13$. The width of the interference field remains of the order of d at distance Z_d.

The detector at distance Z_d consists of a CsI-coated, two-microchannel-plate (MCP) assembly (mounted in series), coupled to a phosphor screen on which the fringe pattern is imaged with a charge-coupled-device (CCD) camera. The two-stage MCP+phosphor screen have an overall spatial resolution of 90 μm, which would not suffice to resolve the fringe spacing. They are therefore tilted so that the incident beam makes a grazing angle of 8° with respect to the CsI input plan, and the fringe spacing is magnified by a factor of 7 up to 450 μm. For determining the resolution of the whole system at the harmonic wavelength, we produce a known, regular intensity pattern by using a calibrated mesh as a mask on the first microchannel plate. The response function of the detector can be deduced from the measured pattern. We find that the measured fringe contrast (the spatial degree of coherence) should be multiplied by 1.7 to compensate for the MCP response. After they are tilted, the MCP's still have sufficient gain to obtain single-shot pictures.

III. DETERMINATION OF THE DEGREE OF SPATIAL COHERENCE

We have measured interference patterns at three distances Z_d after the interferometer, i.e., for three separations d in the incident beam. Figure 2 shows two-dimensional interferograms, where x and y are horizontal and vertical dimensions, obtained for $Z_d = 1$, 2, and 3 m, i.e., $d = 1$, 2, and 3 mm, respectively, and their characteristic profiles along the x axis. The angle of the fringes with the vertical (38°) comes from a slight misalignment (0.6°) of the mirrors relative to the incident beam. In all cases, well-contrasted fringes are obtained, indicating a good spatial coherence over 3 mm. At a distance $Z_d = 1$ m [Fig. 2(a)], the width of the interference field is $d = 1$ mm, so that a small number of fringes is produced. At a

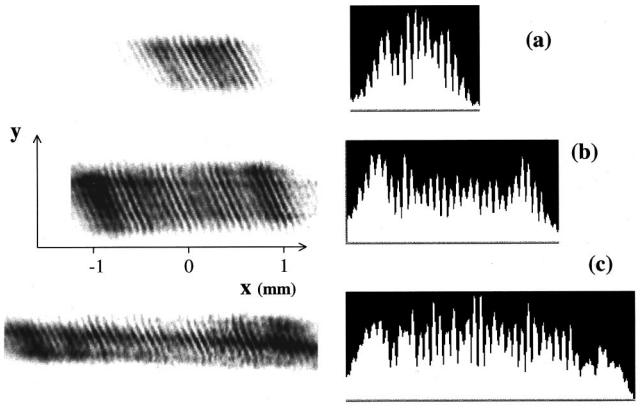

FIG. 2. Two-dimensional interferograms at distances (a) $Z_d = 1$ m, i.e., for a separation $d = 1$ mm between the interfering rays in the incident beam, jet-to-focus position $z = +40$ mm (jet after focus for positive abscissa), backing pressure $P = 1000$ Torr; (b) $Z_d = 2$ m, $d = 2$ mm, $z = +80$ mm, and $P = 1000$ Torr; and (c) $Z_d = 3$ m, $d = 3$ mm, $z = +40$ mm, and $P = 400$ Torr.

distance $Z_d = 2$ m [Fig. 2(b)], the two halves of the incident beam have clearly crossed and overlapped almost symmetrically. The interference field width and the number of fringes are doubled. The structures on both sides of the profile are enhanced due to the diffraction by the central edge of the mirrors. At a distance $Z_d = 3$ m [Fig. 2(c)], the contrast is still large in the central part of the profile, where, for almost symmetric rays in the two half-beams, the interfering electric fields have equal amplitudes. The contrast is weaker on the sides where the electric fields along asymmetric rays interfere with different amplitudes. Note that all interferograms in Fig. 2 result from the superposition of two fringe patterns for wavelengths $H13$ (61.53 nm) and $H15$ (53.33 nm), and thus have slightly different spacings. A beat modulation of the contrast is indeed clearly visible, especially in the profile at $Z_d = 2$ m. In order to extract the spatial coherence of the harmonic beam from the interferograms as simply as possible, we have grounded our analysis on the following simplifying remarks and assumptions.

Resolving diffraction and interference effects

First we note in the profiles of Fig. 2 that Fresnel diffraction by the mirror edge should affect the intensity distribution of each half-beam in the x dimension. The peak intensity on each side is enhanced, whereas the pseudoperiodical modulation is hardly apparent. Diffraction also occurs in the y dimension, as it is visible in the interferogram for $Z_d = 2$ m (horizontal lines); this is due to the limited vertical aperture of the interferometer. Nonetheless, we assume (assumption 1) that diffraction should not significantly affect the interference, i.e., the contrast of the fringes throughout the interferogram. More precisely, we claim that the fringe analysis can be separated from the description of the diffraction. It is clear that vertical diffraction only results in modulating each line by the same factor; that is, there is no change in the contrast. To illustrate the case of the horizontal diffraction, in Fig. 3(a) we show a spatial profile $I_d(x,y)$ along

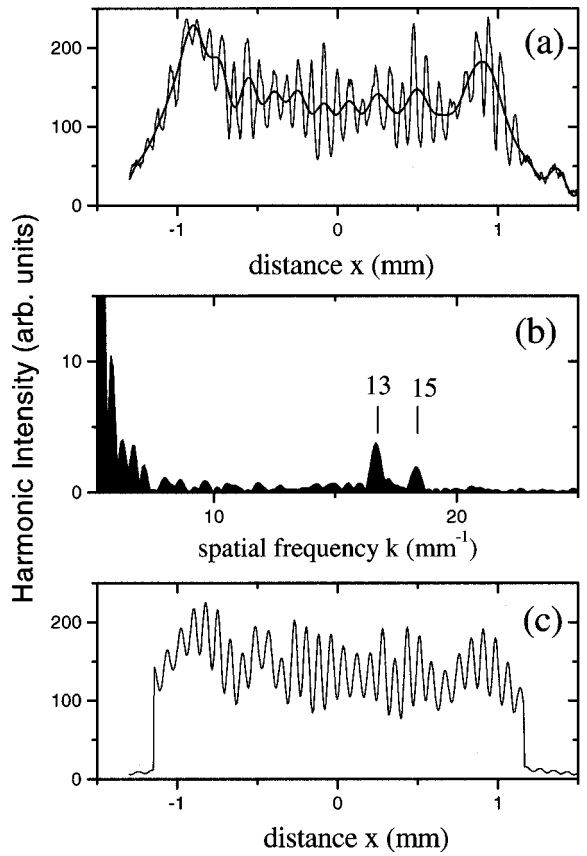

FIG. 3. (a) 1D profile along the x dimension of the measured $I_d(x,y)$ 2D interferogram at a distance $Z_d=2$ m ($d=2$ mm); the reconstructed profile including only diffraction by the mirror's edge is superimposed. (b) Fourier transform $F[I_d](k)$ of the $I_d(x,y)$ profile as a function of the x-conjugate spatial frequency k; the low-frequency part of the spectrum corresponds to diffraction by the mirror's edge—the two peaks at $k_{13}=16.5\,\mathrm{mm}^{-1}$ and $k_{15}=18.5\,\mathrm{mm}^{-1}$ are clearly resolved. (c) Reconstructed 1D-profile along the x dimension, including interference with a measured γ_d degree of coherence and diffraction; it compares reasonably with the experimental profile (*a*).

x in the interferogram for $Z_d=2$ m (thin line), and in Fig. 3(b) the Fourier transform $F[I_d](k)$ of I_d with respect to x. The signal $F[I_d](k)$ presents two clearly distinct regions of spatial frequencies. On the one hand, it exhibits two well-resolved peaks at spatial frequencies $k_{13}=2\pi\alpha/\lambda_{13}$ and k_{15}, corresponding to $H13$ and $H15$ fringe patterns, respectively. The ratio 1:3 of the amplitudes for $H15$ and $H13$ components reflects their relative contributions to the harmonic beam. On the other hand, the low part of the spectrum, between 0 and 50 in Fig. 3(b), corresponds to the long-range variation of the intensity profile, i.e., of Gaussian type including diffraction. After suppression of the high components at k_{13} and k_{15} in the spectrum $F[I_d]$, we perform an inverse Fourier transform to rebuild the profile which is plotted in Fig. 3(a) (thick line), including only the diffraction effects. It displays a typical pseudoperiodical modulation of the Fresnel diffraction. Conversely, information on the fringe pattern is all contained in the high-frequency part of the $F[I_d]$ spectrum. Starting from an analytical representation of the Fresnel diffraction of a Gaussian profile, we checked that the amplitude in the Fourier spectrum was negligible at the k_{13} frequency of the fringes. By means of this clear partition and simple operations on $F[I_d]$ spectrum, we can analyze either diffraction or the interference of the two half-beams.

Two-dimensional mapping of the degree of spatial coherence

Thanks to the separation between the diffraction and interference, we now describe the interference state at point $Q(Z_d,x)$ in the usual simple way as a sum of two geometrical rays issued from P_1 and P_2, respectively, separated by d in the transverse cross section of the incident beam. Denoting $E(P_1;t)e^{i\varphi(P_1;t)}$ the electric field (modulus and phase) at $P_1(P_2)$, we recall that the complex degree of spatial coherence $\gamma(P_1,P_2)$ between the fields at P_1 and P_2 is expressed as

$$\gamma(P_1,P_2)=\gamma_{12}e^{i\alpha(P_1P_2)}=\frac{\langle E(P_1;t)E(P_2;t)e^{i\Delta\varphi(P_1,P_2;t)}\rangle}{\sqrt{\langle E(P_1;t)^2\rangle\langle E(P_2;t)^2\rangle}}, \tag{1}$$

where $\Delta\varphi(P_1,P_2;t)$ is the phase difference, and the brackets denote the time average over the pulse duration. The $\gamma(P_1,P_2)$ degree depends *a priori* on the absolute positions of P_1 and P_2 in the incident beam. Under the geometrical condition that the two rays interfere in Q, the coordinates of P_1 and P_2 can be expressed in terms of x, y, and d. Under further condition that the time $(P_1Q-P_2Q)/c$ is negligible, the fringe pattern profile $I_d(x,y)$ relative to the wavelength $H13$ can be written as

$$I_d(x,y)=I_{1d}(x,y)+I_{2d}(x,y)+2\gamma_d(x,y)\sqrt{I_{1d}(x,y)I_{2d}(x,y)}\times\cos[k_{13}x+\alpha(P_1P_2)]. \tag{2}$$

In Eq. (2), $I_{1d}(x,y)(I_{2d})$ is the intensity 2D distribution in the harmonic half-beam reflected by mirror 1 (2), including diffraction by the mirror edge. In order to have a first estimate of γ_d, and to look at its eventual variations in space, we have performed the following local analysis. To start with, we build the I_d map relative to $H13$, by skipping the modulation at the k_{15} spatial frequency in the experimental map in Fig. 2, using line-to-line spatial frequency filtering in the Fourier domain. We then obtain a determination of the local $\gamma_d(\overline{x},y)$ at the coarse abscissa $\overline{x}$ using Eq. (2):

$$\gamma_d(\overline{x},y)=\frac{I_d^{\max}-I_d^{\min}}{4\sqrt{I_{1d}I_{2d}}}. \tag{3}$$

In Eq. (3), $I_d^{\max}$ and $I_d^{\min}$ are the maximum and minimum of the I_d mapping close to $\overline{x}$, for y fixed. The intensity distributions I_{1d} and I_{2d} are obtained line by line, from a fit of the interference-free profile, including only the diffraction in Fig. 3(a). For achieving the fit we choose a reasonable description of $I_{1d}(I_{2d})$: it is computed analytically as an approximate form of the Fresnel diffraction, at a distance $Z_d=d/\alpha$ of a Gaussian amplitude $I_0^{1/2}\exp(-x^2/w^2)$, incident on the bimirror and centered on the mirror edge [11]. The pa-

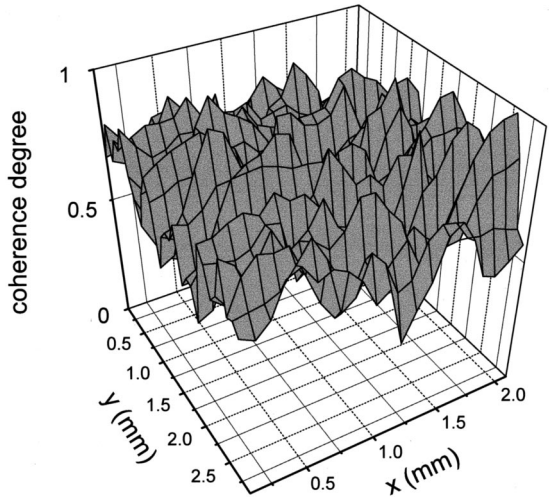

FIG. 4. 2D map of the $\gamma_d(x,y)$ degree of spatial coherence determined from a point-to-point analysis of the 2D interferogram at a distance $d=2$ mm, a jet-to-focus position $z=+80$ mm, and a backing pressure $P=1000$ Torr. x and y dimensions have an extension close to 2 mm. The rather uniform $\gamma_d(x,y)$ fluctuates around 0.6.

rameters I_0 and w, the half width at $1/e$ of the amplitude distribution, are free in the fit. We find $2w$ (the full width at $1/e^2$ of the intensity distribution) close to 3 mm, which corresponds to the value expected from the beam divergence. The resulting $\gamma_d(\overline{x},y)$ in Eq. (3) is mapped in Fig. 4 for $Z_d=2$ m; the conditions of harmonic generation are defined in the figure caption. γ_d is rather uniform as a function of y; we note that the y-vertical range of ≈ 2 mm in Fig. 4 is smaller than the $2w$ width of the intensity distribution. Moreover, it does not show a noticeable variation with x except on the left and right sides of the map. On these sides, the rays interfere with very different amplitudes, e.g., I_{1d} maximum and I_{2d} small, so that the normalization by I_{2d} in Eq. (3) introduces a large uncertainty. As a rule, the γ_d degree fluctuate slightly around an average value of 0.6, with a standard deviation of 0.06. Note that the regular fringe pattern in Fig. 2 has already shown that the phase $\alpha(P_1P_2)$ of the complex coherence degree should essentially be constant throughout the map. The same type of rather uniform map is obtained for various conditions of harmonic generation. This is in contrast with the results reported in Ref. [9], where, surprisingly enough, a significant increase of the γ_d was measured as the pair of rays moves from symmetrical to very asymmetrical relative positions in the incident beam. In our case, we assume (assumption 2) that it is reasonable to compute the number $\gamma_d=\langle\gamma_d(\overline{x},y)\rangle$, $\overline{x}$ and y averaged over the full interferogram. This characterizes with one single number the average correlation between all the pairs of rays separated by d in the incident beam.

Averaged degree of spatial coherence from Fourier analysis

Under assumptions 1 and 2, we have performed a second type of analysis where the averaged γ_d is computed from the Fourier spectrum $F[I_d]$ rather than the spatial spectrum I_d.

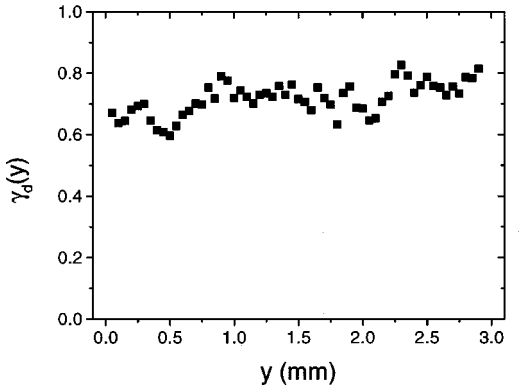

FIG. 5. $\gamma_d(y)$ degree of spatial coherence averaged over the x dimension, determined from Fourier analysis of the 2D interferogram at $d=2$ mm, a jet-to-focus position $z=+80$ mm, and a backing pressure $P=1000$ Torr. As in Fig. 4, $\gamma_d(y)$ slightly fluctuates around 0.7, so that the y-averaged value γ_d can be computed to characterize the spatial coherence with a single number.

We now write Eq. (2) with $\gamma_d(y)$ independent of x, but formally keeping its dependence on y. We ignore diffraction so that I_{1d} and I_{2d} are now purely Gaussian functions. At a distance Z_d, the two half-beam maximums are separated by d, so that $I_{1d}(x)$ is centered at $x=-d/2$ ($x=+d/2$ for I_{2d}):

$$I_{1d}(x)=I_0e^{-2(x+d/2)^2/w^2}Y(x+d/2), \tag{4}$$

where $Y(x)$ is the Heaviside function. The parameters I_0 and w have been fixed from the fit of the interference-free profile, as previously explained. Except for $\gamma_d(y)$, the y dependence of the line-to-line analysis is implicit. The Fourier transform $F[I_d](k)$ of I_d in Eq. (2), using the expression in Eq. (4), can be calculated analytically. We simply obtain $\gamma_d(y)$ by identifying the $F[I_d](k)$ expression at spatial frequency $k=k_{13}$ to the measured number in the profile in Fig. 3(b):

$$\gamma_d(y)\approx\frac{\sqrt{2}F[I_d](k_{13})}{w\sqrt{\pi}I_0\,\mathrm{erf}\left(\dfrac{d}{\sqrt{2}w}\right)}e^{d^2/2w^2}. \tag{5}$$

The determination of $\gamma_d(y)$ from the Fourier spectrum in Eq. (5) allows one to filter the noise: this is equivalent to averaging the fringe-to-fringe determination in Eq. (3). We check that the parameters I_0 and w and the degree $\gamma_d(y)$ are consistently determined by rebuilding the full profile $I_d(x)$ in Fig. 3(c), close enough to the experimental profile in Fig. 3(a).

The above line-to-line analysis gives $\gamma_d(y)$, which is in good agreement with the $\overline{x}$-averaged value from the 2D analysis. Moreover, the same uniform behavior is measured along the y dimension, as further illustrated in Fig. 5. Therefore, 2D-averaged values of γ_d are now discussed. The full analysis can be performed on a personal computer. This has allowed a systematic study of the spatial coherence of the harmonic beam, requiring the treatment of more than 1000 interferograms.

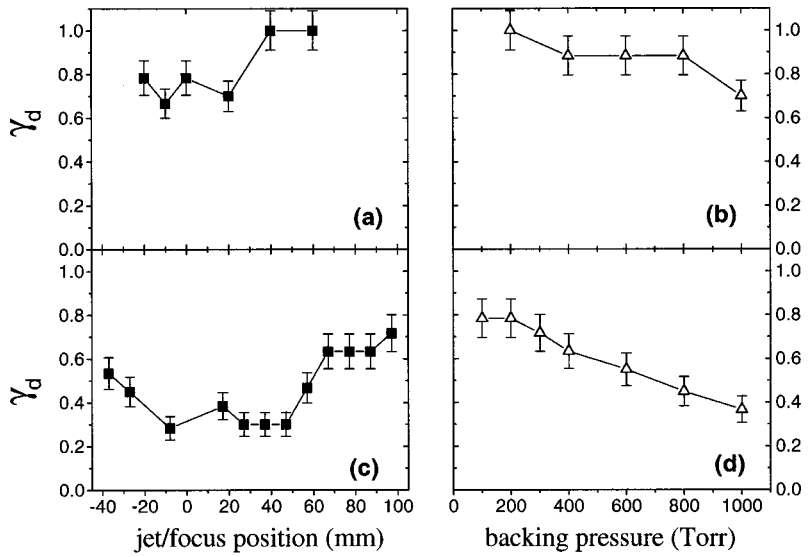

FIG. 6. The 2D-averaged γ_d for $d=1$ mm and 2 mm, as a function of the generation parameters: Backing pressure $P=1000$ Torr (pressure in the jet $\approx P/10$), and γ_d as a function of jet-to-focus position z, [(a) $d=1$ mm, (c) $d=2$ mm]; and $z=-20$ mm, and γ_d as a function of P [(b) $d=1$ mm, (d) $d=2$ mm].

IV. INFLUENCE OF THE GENERATION CONDITIONS

We report in details the determination of the 2D-averaged γ_d for $H13$, at distance $Z_d=1$ and 2 m; that is, for pairs of rays separated by $d=1$ and 2 mm in the incident beam. It is studied as a function of the harmonic generation parameters, namely, (i) the position of the laser focus relative to the gas jet ($z>0$ for a laser focused before the jet), and (ii) the gas pressure in the jet (the pressure in the pulsed jet is typically ten times less than the backing pressure, noted P). Similar but less extended studies, on account of the weaker signal in Fig. 3(b), have been performed for $H15$, but are not reported here. For most of the measurements, the laser peak intensity is close to 2×10^{14} W/cm^2. For given conditions, P and z fixed, we record at least ten single-shot images which are analyzed line by line as described above. The statistical analysis provides the shot-averaged $\gamma_d(y)$, the shot- and 2D-averaged γ_d's and their standard deviations. The overall standard deviation of γ_d is 0.06, of the order of that on $\gamma_d(y)$. This mainly reflects the laser intensity and gas density fluctuations.

The γ_d values are plotted in Fig. 6 as a function of z and P, for $Z_d=1$ and 2 m. For $Z_d=1$ m, i.e., $d=1$ mm, γ_d is larger than or equal to 0.7 in the whole range of parameters. For a fixed pressure $P=1000$ Torr in Fig. 6(a), γ_d increases from 0.7 to 1 as the laser focus is moved away from the jet. For fixed $z=23$ mm in Fig. 6(b), γ_d remains quasiconstant with pressure, although a slight decrease is observed at high pressure (1000 Torr).

For $Z_d=2$ m, i.e., $d=2$ mm, γ_d is larger than or equal to 0.3 in the whole range of parameters. For a fixed pressure $P=1000$ Torr in Fig. 6(c), γ_d increases from 0.3, when the laser beam is focused in the jet, to 0.7 when the laser focus is at $z=100$ mm before the jet. The variation with the xenon density for fixed $z=-20$ mm is also significant in Fig. 6(c): the γ_d value decreases almost linearly from 0.8 at 100 Torr to 0.4 at 1000 Torr. Note that the two variations with z are reported in a range of z values that is not symmetric about 0. Yet the interferograms were recorded while keeping approximately the same gain on the MCP, thus exploring a region of about constant harmonic generation efficiency. The relative position of the laser focus and the gas jet has been measured with an uncertainty of only ±10 mm. A possible explanation for this is the asymmetry of the conversion efficiency due to phase matching, as reported in Ref. [7].

In summary, the harmonic beam presents a good spatial coherence, $\gamma_d\geqslant0.5$, within a cell of diameter 2 mm, in the range $P\leqslant500$ Torr for the backing pressure. The highest coherence, γ_d close to 0.8 in the 2-mm cell, is measured at low pressure and for the laser focus about 100 mm before the medium.

Comparison with an incoherent source

The γ_d values for three distances d are plotted in Fig. 7, for the same conditions of focusing and pressure (P

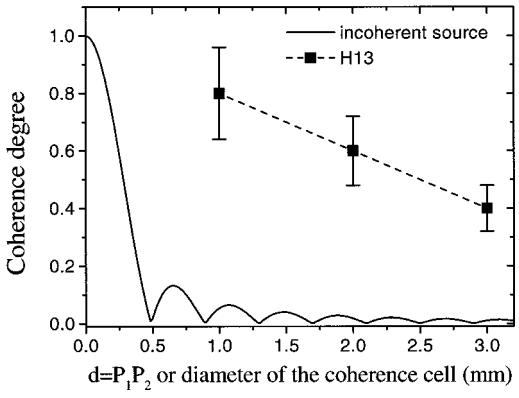

FIG. 7. Comparison of γ_d for the 13th harmonic with that of an incoherent source of the same diameter at distance $D=1300$ mm, as a function of the diameter d of the coherence cell.

$=1000$ Torr, $z=+60$ mm). We recall that we measure the coherence of the harmonic beam not exactly after the source, but after the beam has diverged over a source-spherical mirror distance of 1300 mm and propagated parallel over 2.6 m to the interferometer. We assert that the parallel propagation does not affect the coherence. The diverging propagation changes it slightly, at least at a very short scale in the wave front. According to the van Cittert–Zernike theorem [12], the light emitted from a purely incoherent source of radius ρ will present a given degree of coherence γ_d within a cell of diameter d_{incoh} which increases with the distance D from the source as $d_{\mathrm{incoh}} \equiv \lambda D/\rho$, where the proportionality factor depends on γ_d. An estimate of the size of the harmonic beam at the exit of the jet is given by $\rho=\rho_L/p^{1/2}$, where ρ_L is the laser spot radius and p an effective order of nonlinearity in general smaller than the harmonic order [13]. For harmonic 13, $p\sim 7$ and $\rho_L \sim 250\,\mu$m (the laser beam was diffraction limited between two and three times) give $\rho \sim 100\,\mu$m. In Fig. 7, we compare the measured coherence, at distance $D=1300$ mm from the harmonic source, with the one from an incoherent source of same radius $\rho=100\,\mu$m, as a function of the coherence cell diameter. It is clear from Fig. 7 that for the incoherent source, the coherence cell in which $\gamma_d \geqslant 0.4$ has a diameter $d_{\mathrm{incoh}} \approx 300\,\mu$m, much smaller than the distance $d=3$ mm for which the same degree of correlation is measured in the harmonic beam. Therefore, we actually measure the intrinsic coherence of the harmonics in the experiment. The comparison of the measured coherence with that of the field radiated by an incoherent source of same diameter was also developed in Ref. [9]. Despite the different generating conditions (a harmonic diameter of 70 μm, the laser focused with $r/f=1/100$) and distance where the coherence was probed (only 40 mm away from the generating medium), both comparisons are quite similar. Note, however, that the parameter important in most applications is the coherent flux, i.e., the flux contained in the area where the coherence degree stays above, say, 0.4. We have shown that the latter condition can be met over the full diameter of the harmonic beam (3 mm), which means that all the harmonic flux is coherent. In Ref. [9], the coherence of the 13th harmonic drops to 0.2 for $d=100\,\mu$m, for a full diameter of 350 μm, indicating a loss of coherence certainly due to the ionization conditions.

Discussion: ionization and phase effects

For the purpose of discussion, we consider two points P_1 and P_2 in the harmonic transverse section at the exit of the medium. As clearly explained in Ref. [8], all the processes which cause different time histories of the rays emerging at P_1 and P_2 will lower the spatial coherence between them. We note from definition (1) that $|\gamma(P_1,P_2)|=1$ implies that $E(P_1;t)$ and $E(P_2;t)e^{i\Delta\varphi}$ are proportional everywhere in time, i.e., have exactly the same history. In the case of a cylindrical geometry of the laser beam and medium, this should be the case for symmetrical points. Generally speaking, different histories of the phases already produce a decrease of spatial coherence. In effect, the average values in the Schwarz inequality $|\langle E(P_1;t)E(P_2;t)e^{i\Delta\varphi}\rangle| \leqslant |\langle E(P_1;t)E(P_2;t)\rangle|$ are equal if and only if the phase difference $\Delta\varphi$ is constant everywhere in time. Now, in general, both the modulus and phase of the harmonic field have different histories at the two nonsymmetrical points P_1 and P_2. This is particularly the case when ionization takes place in the generating medium, producing a time-increasing density of electrons which varies substantially from place to place. In the simple ideal case of perfect phase matching, the phase of the harmonic field *in the medium* is equal to the one of the nonlinear polarization. To a first approximation (loosely focused beam, and weakly dispersive medium whose length is small compared to the confocal parameter), it can be expressed as the sum of two terms: (i) the phase $(q\omega/c)\int_0^z n_1(r,z';t)dz'$ of a quasiplane wave where $n_1=\sqrt{1-[N_e(r,z;t)e^2/m\omega^2\varepsilon_0]}$ is the refractive index at frequency ω in the presence of an electron density $N_e(r,z;t)$; and (ii) the intrinsic dipole phase $\varphi_{at}=\eta I_L$, proportional to the laser intensity I_L [5]. The first term (i) should vary with the time-increasing electron density; therefore it should vary differently in time along the rays that emerge in P_1 and P_2, respectively. Actually, due to the radial laser intensity distribution, ionization of the medium is faster on the axis. For term (ii) the difference of the dipole phases $h[I_L(l;t)-I_L(2;t)]$ between any two nonsymmetrical points in the medium is obviously timedependent, which should result in two different histories of the phases in P_1 and P_2. Note that the above discussion implies that, in principle, the degree $\gamma(P_1,P_2)$ varies for a fixed distance $d=P_1P_2$ with the absolute position of the (P_1,P_2) midpoint. This points out that the choice, according to assumption 2 (see Sec. III) of a constant γ_d, which can be determined from the Fourier analysis, should be carefully interpreted. It has the approximate meaning of an average value only when $\gamma(P_1,P_2) \equiv \gamma_d(x,y)$ is slowly varying with x, as is the case in Figs. 4 and 5. In the general case, it should rather be viewed as an effective γ_d.

From the above discussion, the variations of γ_d as a function of the pressure in Figs. 6(b) and 6(d) can certainly be attributed to ionization: the faster and higher the electron density develops in the medium, the higher the decorrelation of the time-dependent fields at the medium end. Now, the variation of γ_d with the laser focus and jet relative positions in Fig. 6(a) and 6(c) can be related to both (i) the strong ionization at the maximum laser intensity close to focus, and (ii) the effect of the dipole phase, which is all the more important as I_L is high. To attempt to unravel the two effects, we have performed a simulation of the 13th harmonic field, and computed the degree of coherence for both near and far fields. The simulation code, which was extensively described in Ref. [7], includes a computation of the nonlinear polarization in the strong-field approximation and the coupled propagation of the fundamental and the harmonic fields in the presence of ionization. In Fig. 8, we plot the averaged γ_d as a function of z, for three different backing pressures (the pressure in the jet is $P/10$), at an intensity of 10^{14} W/cm^2. The γ_d degree actually decreases from 1, when the laser is focused either far before or after the jet, to 0.6, when the focus is at 20–30 mm after the jet. Note that the curve is not

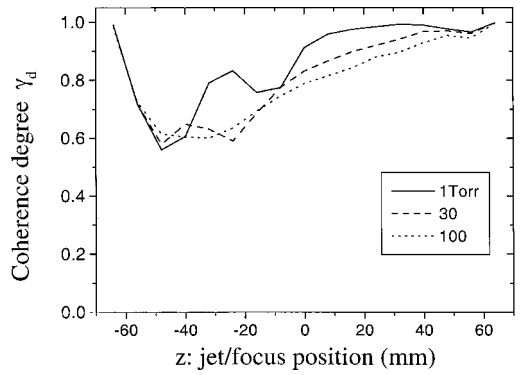

FIG. 8. Calculated degree of spatial coherence for $d=2$ mm, as a function of the jet-to-focus position, for three different backing pressures (the pressure in the jet is $\approx P/10$). Coherence is at a minimum in the focus region even at very low pressure and negligible electron density in the medium. This indicates that coherence is degraded through the intensity-dependent phase of the atomic dipole. The coherence decrease with pressure, i.e., with electron density, occurs first when the jet is after the focus.

symmetrical. The overall variation of the calculated γ_d is compatible with the one measured in Fig. 6(c). The simulation also shows that for a focus position from far before to 15 mm after the jet, γ_d decreases with pressure. The dependence is more irregular at larger z after the jet, where γ_d seems to oscillate slightly with P. Beyond this agreement, the quantitative comparison with the measured γ_d is not perfect. First, the asymmetry in the simulation does not appear as clearly in the measured curve. The calculated value of 0.6 at the curve minimum remains higher than the one in Fig. 6(c). Actually, the laser field is only approximately modeled in the simulation: it is chosen as Gaussian with a confocal parameter $b=120$ mm, whereas it is experimentally close to Gaussian but with $M^2=2$. As a result, the generation in the jet close to focus, where the dependence of the harmonic field with the laser intensity is the most critical, maybe not well enough described in the simulation. Moreover, we do not account for the annular structure of the laser far field: it leads to essentially the same laser field in the focus region as the one resulting from a regular profile, but the difference between annular and regular beams should increase as one moves away from the focus. Both approximations can explain that the z scale is different between the calculated and experimental curves. This could also explain that, whereas the experimental γ_d in Fig. 6(d) as a function of P is measured for a focus 10 mm after the jet, the simulated curves display a poor pressure dependence in this range.

However, an important point can be underlined from the simulation: the dominant part of the variation of the γ_d remains at a very low pressure (backing pressure $P=10\times 1$ Torr), where the electron density plays no role. We thus suggest that in a finite range of negative-z values, the marked decrease of γ_d can be interpreted as a decorrelation of the fields mainly due to the intensity-dependent phase of the atomic dipole. Out of this range, for instance, for z values as in Figs. 6(b) and 6(d), where a variation of γ_d with pressure is clearly measured, the decorrelation should result from both the onset of ionization and the variation of the atomic dipole phase. This could be the true explanation of the decrease of the coherence with intensity observed by Ditmire *et al.*, since this decrease was not found to depend on the backing pressure. In the present experiment, we have not systematically studied γ_d as a function of z for a large set of pressure or laser intensity; further investigation is envisaged.

Comparison with x-ray laser sources

It is of interest to compare the spatial coherence of the harmonic beam to that of the other short pulse XUV sources. Here, we limit the discussion to x-ray laser sources (SXRL's) for which spatial coherence has been reported. These are of two types, depending on whether the plasma is produced on a solid target or in a capillary. In the solid target configuration, intensive studies were performed since the first measurements at 20.6 nm [14]. Several experiments were done using a Young two-slit interferometer with Ne-like SXRL's at 19.6 and 23.2 nm [15,16]. The transverse coherence degree was studied as a function of amplification geometry and temporal region of the pulse [17,18]. A typical value for these experiments is a spatial coherence length close to 100 μm ($\gamma_d \geqslant 0.8$ for $d \leqslant 100\,\mu$m), 1 m away from the source, corresponding to a diameter of about 100 μm of the equivalent incoherent source. This diameter is comparable to that of the plasma source, and it varies similarly. Albert *et al.* measured the intrinsic coherence of SXRL's by analyzing the diffraction by a wire of small diameter [19]. They reported a small value close to 10 μm, which indicates that the coherence of the far field results mainly from the propagation, on account of the high brightness of the SXRL emission. The latter technique has been used in the capillary discharge configuration to measure the coherence length as a function of the capillary length, 6 m away from the source, for a 46.9-nm Ne-like Ar SXRL [20]. The best coherence length of 4.5 mm has been measured for a 164-mm-long capillary. For comparison this would correspond to a coherence length of 750 μm at 1 m from the equivalent incoherent source of diameter 50 μm. This is about three times larger than the coherence obtained from SXRL's on a solid target, but it remains smaller than the intrinsic coherence of the harmonic emission.

V. CONCLUSION

We have measured the degree of spatial coherence γ_d of the 13th harmonic of Ti: sapphire at 800 nm, using a Fresnel-mirrors interferometer. With this system, a two-dimensional mapping of γ_d can be obtained as a function of the distance d between the interfering rays in the incident beam. Analysis of the interferogram is based on an approximation which resolves the interference modulation from the diffraction of the beam by the mirror's edge. A local determination shows that γ_d is rather uniform in the beam section. An averaged value is measured as a function of the relative jet and focus positions and of the backing pressure. As expected, the harmonic coherence is high over the full diameter of the harmonic beam (3 mm at a distance 1300 mm from the gas jet). The γ_d degree remains higher than 0.8 within a cell of 1 mm in diameter, in the full range of focusing position and pres-

sure. It is larger than 0.5 within a cell of 2 mm in diameter for focusing outside the jet and for low enough pressure. The intrinsic coherence of the harmonic is much larger than the one of the x-ray lasers produced on solid targets, which is close to the coherence at a distance from an incoherent source. Coherence is degraded under the two conditions of focusing in the jet and increasing pressure. Both produce enhancement from ionization of a time- and space-dependent electron density, which can affect phase matching and degrade the coherence. Simulations of γ_d lead to a qualitative agreement with the measured values. Nonetheless, they demonstrate that coherence is degraded when focusing in the jet, even at very low pressure where ionization plays no role. This suggests that the intensity-dependent phase of the atomic dipole is an important cause of field decorrelation, that might explain previously reported coherence measurements.

ACKNOWLEDGMENTS

The authors greatly acknowledge G. Jamelot, A. Klisnick, and P. Zeitoun of the LSAI at Orsay, who lent us the Fresnel-mirror interferometer and part of the detector setup; O. Gobert, P. Meynadier, and M. Perdrix in charge of the LUCA laser facility in Saclay, for their highly efficient and kind assistance; and F. Albert for an enlightening discussion of spatial coherence concepts.

[1] D. Joyeux, P. Jaeglé, and A. L'Huillier, in *Trends in Physics* edited by A. Consortini (Academic, London 1996), Vol. 3, p. 371.

[2] J. Peatross and D. D. Meyerhofer, Phys. Rev. A **51**, R946 (1995); **52**, 3976 ().

[3] J. W. G. Tisch, A. R. Smith, J. E. Muffet, M. Ciarocca, J. P. Marangos, and M. H. R. Hutchinson, Phys. Rev. A **49**, R28 (1994).

[4] P. Salières, T. Ditmire, K. S. Budil, M. D. Perry, A. L'Huillier, J. Phys. B **27**, L217 (1994); P. Salières, T. Ditmire, M. D. Perry, A. L'Huillier, and M. Lewenstein, *ibid.* **29**, 4771 (1996).

[5] P. Salières, A. L'Huillier, and M. Lewenstein, Phys. Rev. Lett. **74**, 3776 (1995).

[6] L. Le Déroff, P. Salières, and B. Carré, Opt. Lett. **23**, 1544 (1998).

[7] P. Salières, A. L'Huillier, Ph. Antoine, and M. Lewenstein, Adv. At., Mol., Opt. Phys. **41**, 83 (1999).

[8] T. Ditmire, E. T. Gumbrell, R. A. Smith, J. W. G. Tisch, D. D. Meyerhofer, and M. H. R. Hutchinson, Phys. Rev. Lett. **77**, 4756 (1996).

[9] T. Ditmire, E. T. Gumbrell, R. A. Smith, J. W. G. Tisch, D. D. Meyerhofer, and M. H. R. Hutchinson, Appl. Phys. **65**, 313 (1997).

[10] J. Svatos, D. Joyeux, D. Phalippou, and F. Polack, Opt. Lett. **18**, 1367 (1993).

[11] L. D. Landau and E. M. Lifshitz, *The Classical Theory Fields*, 2nd ed. (Pergamon, Oxford, 1962).

[12] M. Born and E. Wolf, *Principles of Optics* 6th ed. (Cambridge University Press, Cambridge, 1980).

[13] A. L'Huillier, Ph. Balcou, S. Candel, K. J. Schafer, and K. C. Kulander, Phys. Rev. A **46**, 2778 (1992).

[14] J. E. Trebes, K. A. Nugent, S. Mrowka, R. A. London, T. W. Barbee, M. R. Carter, J. A. Koch, B. J. MacGowan, D. L. Matthews, L. B. Da Silva, G. F. Stone, and M. D. Feit, Phys. Rev. Lett. **68**, 588 (1992).

[15] R. E. Burge, G. E. Slark, M. T. Browne, X.-C. Yuan, P. Charalambous, Z. An, X.-H. Cheng, C. L. S. Lewis, A. G. MacPhee, and D. Neely, J. Opt. Soc. Am. B **14**, 2742 (1997).

[16] P. Lu, E. Fill, Y. Li, J. Maruhn, and G. Pretzler, Phys. Rev. A **58**, 628 (1998).

[17] R. E. Burge, G. E. Slark, M. T. Browne, X.-C. Yuan, P. Charalambous, X.-H. Cheng, C. L. S. Lewis, G. F. Cairns, D. Neely and A. G. MacPhee, J. Opt. Soc. Am. B **15**, 2515 (1998).

[18] R. E. Burge, G. E. Slark, M. T. Browne, X.-C. Yuan, P. Charalambous, Z. An, X.-H. Cheng, C. L. S. Lewis, A. G. MacPhee, and D. Neely, J. Opt. Soc. Am. B **15**, 1620 (1998).

[19] F. Albert, B. Rus, Ph. Zeitoun, A. Carillon, P. Jaeglé, G. Jamelot, A. Klisnick, D. Ros, and S. Sebban, *X-Ray Lasers 96* (Institute of Physics, Bristol, 1996)

[20] M. C. Marconi, J. L. A. Chilla, C. H. Moreno, B. R. Benware, and J. J. Rocca, Phys. Rev. Lett. **79**, 2799 (1997).